



Three-Dimensional Orientation Mapping in the Transmission Electron Microscope

H. H. Liu, et al. Science **332**, 833 (2011); DOI: 10.1126/science.1202202

This copy is for your personal, non-commercial use only.

If you wish to distribute this article to others, you can order high-quality copies for your colleagues, clients, or customers by clicking here.

Permission to republish or repurpose articles or portions of articles can be obtained by following the guidelines here.

The following resources related to this article are available online at www.sciencemag.org (this infomation is current as of May 12, 2011):

Updated information and services, including high-resolution figures, can be found in the online version of this article at:

http://www.sciencemag.org/content/332/6031/833.full.html

Supporting Online Material can be found at:

http://www.sciencemag.org/content/suppl/2011/05/11/332.6031.833.DC1.html

This article **cites 10 articles**, 1 of which can be accessed free: http://www.sciencemag.org/content/332/6031/833.full.html#ref-list-1

This article appears in the following **subject collections**: Materials Science

http://www.sciencemag.org/cgi/collection/mat_sci

- 5. Y. J. Kim, R. Busch, W. L. Johnson, A. J. Rulison, W. K. Rhim, Appl. Phys. Lett. 65, 2136 (1994).
- 6. X. H. Lin, W. L. Johnson, W. K. Rhim, Mater. Trans. Jpn. Inst. Metals 38, 473 (1997).
- 7. W. L. Johnson, MRS Bull. 24, 42 (1999).
- 8. A. Inoue, Acta Mater. 48, 279 (2000).
- 9. G. Duan et al., Adv. Mater. (Deerfield Beach Fla.) 19, 4272 (2007).
- 10. A. Wiest, J. S. Harmon, M. D. Demetriou, R. D. Conner, W. L. Johnson, Scr. Mater. 60, 160 (2009).
- 11. J. Schroers, Q. Pham, A. Peker, N. Paton, R. V. Curtis, Scr. Mater. 57, 341 (2007).
- 12. Y. Saotome, Y. Noguchi, T. Zhang, A. Inoue, Mater. Sci. Eng. A 375-377, 389 (2004).
- 13. G. Kumar, H. X. Tang, J. Schroers, Nature 457, 868
- 14. G. Kumar, A. Desai, J. Schroers, Adv. Mater. (Deerfield Beach Fla.) 23, 461 (2010).
- 15. J. Schroers, Adv. Mater. (Deerfield Beach Fla.) 22, 1566
- 16. C. D. Han, Rheology and Processing of Polymeric Materials: Polymer Processing (Oxford Univ. Press, Oxford, 2007).
- 17. H. J. Güntherodt, Adv. Solid State Phys. 17, 25 (1977).
- 18. S. R. Nagel, Phys. Rev. B 16, 1694 (1977).

- 19. W. H. Wang, L. L. Li, M. X. Pan, R. J. Wang, Phys. Rev. B 63, 052204 (2001).
- 20. J. Schroers, A. Masuhr, W. L. Johnson, R. Busch, Phys. Rev. B 60, 11855 (1999).
- 21. Y. J. Kim, R. Busch, W. L. Johnson, A. J. Rulison, W. K. Rhim, Appl. Phys. Lett. 68, 1057 (1996).
- 22. J. Schroers, W. L. Johnson, R. Busch, Appl. Phys. Lett. 77, 1158 (2000).
- D. E. Ballard, P. G. Frischmann, A. I. Taub, U.S. Patent 5,005,456 (1991).
- 24. M. R. I. Gibbs, D. H. Lee, I. E. Evetts, IEEE Trans, Maan,
- 20. 1373 (1984). 25. A. Zaluska, H. Matyja, Int. J. Rapid Solidif. 2, 205 (1986).
- 26. T. Kulik, H. Matyja, Mater. Sci. Eng. A 133, 232 (1991).
- 27. M. F. de Oliveira, W. J. Botta, C. S. Kiminami, A. Inoue, A. R. Yavari, Appl. Phys. Lett. 81, 1606 (2002).
- 28. A. R. Yavari, M. F. de Oliveira, C. S. Kiminami, A. Inoue, W. J. F. Botta, Mater. Sci. Eng. A 375-377, 227
- 29. G. Lohöfer, G. Pottlacher, Int. J. Thermophys. 26, 1239
- 30. R. Busch, Y. J. Kim, W. L. Johnson, J. Appl. Phys. 77, 4039 (1995)
- 31. J. Lu, G. Ravichandran, W. L. Johnson, Acta Mater. 51,

- 32. G. J. Dienes, H. F. Klemm, J. Appl. Phys. 17, 458 (1946).
- 33. T. A. Waniuk, R. Busch, A. Masuhr, W. L. Johnson, Acta Mater. 46, 5229 (1998).
- 34. A. Masuhr, T. A. Waniuk, R. Busch, W. L. Johnson, Phys. Rev. Lett. 82, 2290 (1999).
- 35. G. J. Fan, H.-J. Fecht, E. J. Lavernia, Appl. Phys. Lett. 84, 487 (2004)
- 36. H. Choi-Yim, R. Busch, W. L. Johnson, J. Appl. Phys. 83, 7993 (1998).
- Acknowledgments: The authors acknowledge partial support by the II-VI Foundation, the assistance of R. Overstreet with the thermal imaging unit, and useful discussions with M. A. Nicolet. A patent filed by the California Institute of Technology is currently pending. The U.S. patent application number is US2009/0236017 A1.

Supporting Online Material

www.sciencemag.org/cgi/content/full/332/6031/828/DC1 Materials and Methods Figs S1 and S2 References

We describe here a technique for 3D orientation mapping in the TEM (3D-OMiTEM) with

7 December 2010; accepted 1 April 2011 10.1126/science.1201362

Three-Dimensional Orientation Mapping in the Transmission Electron Microscope

H. H. Liu, S. Schmidt, H. F. Poulsen, A. Godfrey, Z. Q. Liu, J. A. Sharon, X. Huang 1,5*

Over the past decade, efforts have been made to develop nondestructive techniques for three-dimensional (3D) grain-orientation mapping in crystalline materials. 3D x-ray diffraction microscopy and differential-aperture x-ray microscopy can now be used to generate 3D orientation maps with a spatial resolution of 200 nanometers (nm). We describe here a nondestructive technique that enables 3D orientation mapping in the transmission electron microscope of mono- and multiphase nanocrystalline materials with a spatial resolution reaching 1 nm. We demonstrate the technique by an experimental study of a nanocrystalline aluminum sample and use simulations to validate the principles involved.

any materials are polycrystalline, meaning that they are composed of a large **▲**number of grains (crystallites) of different crystallographic orientations. A full threedimensional (3D) orientation mapping of such polycrystalline grain structures (with information about the position, size, morphology, and orientation of each grain, as well as the topological connectivity between the grains) is needed to re-

can be obtained with the 3D electron backscatter diffraction technique (3D-EBSD) (1). This technique has a spatial resolution of ~20 nm, but it requires serial sectioning of the sample as part of the data collection process and, thus, is destructive. Recently, two nondestructive 3D x-ray techniques that have a spatial resolution of, at best, 200 nm (2, 3) have been demonstrated. Electron tomography has been used to determine the shape of isolated crystals with a resolution down to 1 nm, but this method cannot be used to obtain orientation maps (4). Furthermore, several approaches (5-10) have been developed for 2D orientation mapping in the transmission electron microscope (TEM). In these approaches, the crystal orientation is determined from diffraction patterns that are either recorded directly using the diffraction mode (5-7) or reconstructed indirectly from conical-scanning dark-field images (8-10). These 2D methods are relevant when the specimen thickness is smaller than the size

late the structure to properties. Such information of the grains.

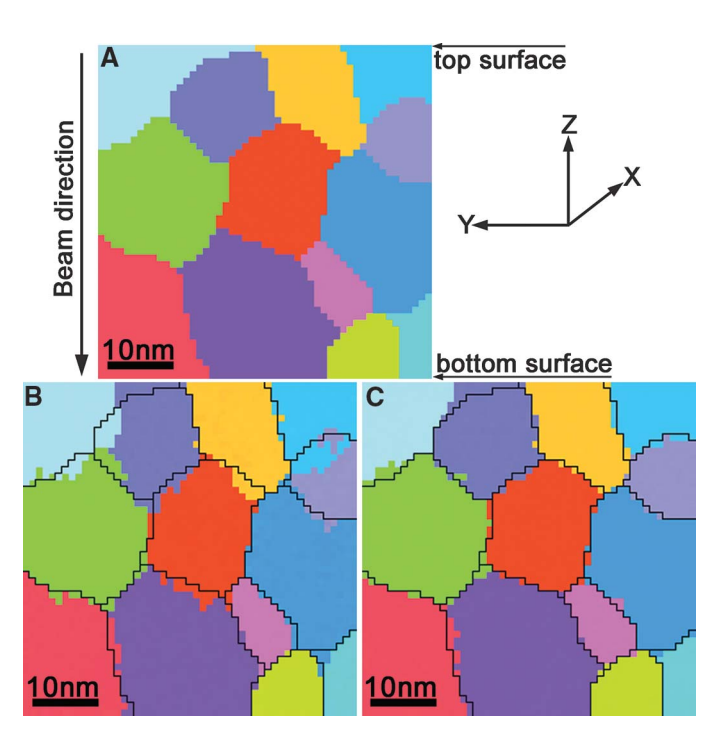
a spatial resolution on the order of 1 nm for specimens that may be substantially thicker than the average grain size. Similar to some of the 2D techniques (8-10), the data collection is based on conical-scanning dark-field imaging. However, to enable the simultaneous reconstruction of a complete 3D orientation map of all grains in a sample volume, images are recorded at many sample tilt angles. Furthermore, we have developed a new approach for the orientation determination and 3D reconstruction, based on the GrainSweeper (11) and GrainSpotter (12) algorithms originally developed for 3D reconstruction of synchrotron diffraction data. In this approach, the orientation of each voxel in the sample is determined by a simultaneous analysis of all contributing diffraction vectors derived from the dark-field images over all beam and sample tilt positions, thereby reducing the effects caused by dynamical diffraction and multiple scattering. A volume formed by adjacent voxels of the same orientation is identified as a grain. The shape and location of each grain are determined with the use of a ray-tracing method based on the sample tilt angles where the grain is visible in the dark-field images. The angular resolution for the orientation mapping is primarily determined by the step sizes used for the conical scanning and the sample tilting, whereas the spatial resolution is also determined by the magnification used to record the images. In general, however, more than 100,000 images are required to obtain nanoscale orienta-

To validate the principles of all procedures involved in the data analysis, we used a software package that incorporates dynamical diffraction and multiple scattering effects (13) to simulate electron diffraction from overlapping grains of different orientations. This package was used in combination with a 3D grain-orientation map

¹Center for Fundamental Research: Metal Structures in Four Dimensions, Materials Research Division, Risø National Laboratory for Sustainable Energy, Technical University of Denmark, DK-4000 Roskilde, Denmark. ²Laboratory of Advanced Materials, Department of Materials Science and Engineering, Tsinghua University, 100084 Beijing, P.R. China. ³Shenyang National Laboratory for Materials Science, Institute of Metal Research, Chinese Academy of Sciences, 110016 Shenyang, P.R. China. ⁴Department of Mechanical Engineering, Johns Hopkins University, Baltimore, MD 21218, USA. 5Danish-Chinese Center for Nanometals, Materials Research Division, Risø National Laboratory for Sustainable Energy, Technical University of Denmark, DK-4000 Roskilde, Denmark

*To whom correspondence should be addressed. E-mail: xihu@risoe.dtu.dk

Fig. 1. (A) Section of a rescaled experimentally obtained 3D-EBSD grainorientation map of aluminum. The tilt axis is parallel to the x axis. (B) Reconstructed grainorientation map for the same section based on a sample tilt range of $\pm 60^{\circ}$. (**C**) Reconstructed grain-orientation map for the same section based on a sample tilting range of $\pm 90^{\circ}$. The same color coding, representing crystallographic orientation, is used throughout. The black lines in (B) and (C) indicate the grain boundary positions in the original map (A).



of an aluminum polycrystal experimentally generated using 3D-EBSD to simulate a set of darkfield images over a wide range of specimen and beam tilt angles. The original grain size of the aluminum sample is 2 µm, which is scaled down by a factor of 100 to simulate a nanocrystalline sample with grains of an average size of 20 nm at a voxel resolution of 1 nm³. Figure 1A shows a section through this "original" grain-orientation map used as the input for the simulations. The vertical direction is parallel to the sample thickness direction, giving up to five overlapping grains in the through-thickness direction. We performed two simulations that generated conical-scanning dark-field images over sample tilt angle ranges of ±60° and ±90°, in each case with a step size of 1°. These dark-field images were then used as input data for the 3D-OMiTEM software. Figure 1, B and C, shows the reconstructed grain-orientation maps for the same section, for the two cases. The black lines superposed on Fig. 1, B and C, indicate the grain boundary positions in the original map (Fig. 1A). The mean mismatch error is 0.9 pixels (0.9 nm) and 0.5 pixels (0.5 nm) in the two cases, respectively. The orientation difference for each grain between the reconstructed maps (Fig. 1, B and C) and the original map (Fig. 1A) is less than 0.2°. The good match in both the grain orientations and the grain boundary locations suggests that the algorithms used for the data collection and analysis in the 3D-OMiTEM method are valid.

We demonstrate the 3D-OMiTEM technique by generating a 3D grain-orientation map of a sample of nanocrystalline aluminum. An aluminum film of 150-nm thickness was produced by pulsed electron beam evaporation (14). 2D observations from the surface plane and cross section

revealed the film to be composed of a mixture of elongated grains and smaller equiaxed grains. Using a tilt range from -30° to $+30^{\circ}$, about 110,000 dark-field images were generated from a selected area of 850 by 850 nm² (14). Part of a 3D grainorientation map reconstructed using the new technique is shown in Fig. 2. More than 100 grains with a wide spectrum of crystallographic orientations are identified. The 3D shapes of many grains are revealed as elongated, but equiaxed grains of smaller sizes embedded in the analyzed volume are also found, in good agreement with the 2D observations. Based on a comparison of the reconstructed grain structure with the darkfield images of individual grains, the resolution of the technique is estimated to be ~two to three pixels (for the magnification range typically used for analysis of nanocrystalline materials, one pixel corresponds to 0.2 to 2 nm).

The volume that can be mapped using 3D-OMiTEM is determined by the TEM sample thickness, which is typically 100 to 300 nm in foils examined at standard operating voltages (200 to 300 kV) and up to 1 µm in 1-MeV instruments, and by the electron illuminated area, which can be as large as several tens of square micrometers, depending on the magnification used in the microscope. For a nanocrystalline material with a grain size of 30 nm in a sample of thickness 200 nm and at a magnification giving a resolution of 1 nm, there will be on the order of 10,000 grains in the analyzed volume, providing good statistics of 3D structural parameters. The ability to observe changes in grain structure in the interior of nanocrystalline samples under conditions such as variable stress and temperature will yield information on materials behavior with minimized surface effects and will allow, for the first time, direct testing of physically based

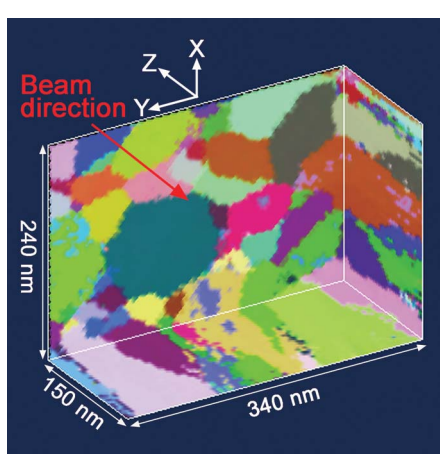


Fig. 2. 3D grain-orientation map from part of a 150-nm-thick aluminum film specimen. The colors represent different crystal orientations with a tolerance of 2° .

models of 3D structural evolution in nanocrystalline materials.

References and Notes

- A. D. Rollett, S. B. Lee, R. Campman, G. S. Rohrer, Annu. Rev. Mater. Res. 37, 627 (2007).
- H. F. Poulsen, Three Dimensional X-Ray Diffraction Microscopy (Springer, Berlin, 2004).
- B. C. Larson, W. Yang, G. E. Ice, J. D. Budai, J. Z. Tischler, Nature 415, 887 (2002).
- P. A. Midgley, R. E. Dunin-Borkowski, Nat. Mater. 8, 271 (2009).
- J.-J. Fundenberger, A. Morawiec, E. Bouzy, J. S. Lecomte, Ultramicroscopy 96, 127 (2003).
- 6. E. R. Rauch, A. Duft, *Mater. Sci. Forum* **495-497**, 197
- K. J. Ganesh, M. Kawasaki, J. P. Zhou, P. J. Ferreira, *Microsc. Microanal.* 15, 752 (2009).
- 8. D. J. Dingley, Microchim. Acta 155, 19 (2006).
- 9. G. L. Wu, S. Zaefferer, *Ultramicroscopy* **109**, 1317 (2009).
- 10. www.cmu.edu/news/archive/2009/June/june4_barmak.shtml
- 11. S. Schmidt et al., Scr. Mater. 59, 491 (2008).
- S. Schmidt, http://sourceforge.net/apps/trac/fable/wiki/ grainspotter.
- K. Sugio, H. H. Liu, H. F. Poulsen, X. Huang, Nanostructured Metals – Fundamentals to Applications, J.-C. Grivel et al., Eds. (Risø DTU, Roskilde, 2009), pp. 337–342.
- Materials and methods are available as supporting material on *Science* Online.

Acknowledgments: We thank K. Sugio for the development of software simulating electron diffraction; E. Johnson, B. Ralph, R. Gardner, H. O. Sørensen, R. Dunin-Borkowski, D. Juul Jensen, N. Hansen, and K. J. Hemker for helpful discussions; and J. R. Bowen and N. Saowadee for providing the 3D-EBSD data. Financial support was provided by the Danish National Research Foundation. A.G. acknowledges support from the National Natural Science Foundation of China under contract numbers 50571049 and 50911130230, Z.Q.L. acknowledges support from the National Basic Research Program of China (grant no. 2010CB631006), and J.A.S. acknowledges support for the thin-film deposition from the U.S. Department of Energy under grant number DE-FGO2-07ER46437.

Supporting Online Material

www.sciencemag.org/cgi/content/full/332/6031/833/DC1 Materials and Methods Reference 15

27 December 2010; accepted 1 April 2011 10.1126/science.1202202